

# Quantum Chemical Study of the Electron-Transfer-Catalyzed Splitting of Oxetane and Azetidine Intermediates Proposed in the Photoenzymatic Repair of (6–4) Photoproducts of DNA

Yinsheng Wang, Peter P. Gaspar, and John-Stephen Taylor\*

Contribution from the Department of Chemistry, Washington University, One Brookings Drive, St. Louis, Missouri 63130

Received June 29, 1999. Revised Manuscript Received February 18, 2000

**Abstract:** Semiempirical AM1 and PM3 calculations were used to study the electron-transfer-catalyzed splitting of oxetanes and azetidines that have been proposed as intermediates in the photoenzymatic repair of the (6–4) photoproducts of dipyrимidine sites in DNA by (6–4) photolyase. The calculations show that the gas-phase splitting of an anion radical to a product complex is more exothermic than that of a cation radical, and that both are more exothermic than the neutral pathway. Low-energy pathways for splitting were found to occur by nonconcerted, two-step mechanisms for both anion and cation radical pathways, but only the anion radicals had lower rate-determining barriers for splitting than did the neutral species. In the anion radical pathway, which is thought to be followed by the enzymatic reaction, cleavage of the C<sub>5</sub>–O<sub>4'</sub> or C<sub>5</sub>–N<sub>4'</sub> bond followed by cleavage of the C<sub>6</sub>–C<sub>4'</sub> bond is more favorable kinetically than cleavage in the reverse order. Though the barrier for cleaving the C<sub>5</sub>–N<sub>4'</sub> bond first is significantly higher for the radical anion of the azetidine than that for cleaving the C<sub>5</sub>–O<sub>4'</sub> bond of the oxetane, protonation of the azetidine nitrogen of the radical anion leads to spontaneous cleavage of the C<sub>5</sub>–N<sub>4'</sub> bond. In the cation radical pathway, cleavage of the C<sub>6</sub>–C<sub>4'</sub> bond followed by cleavage of the C<sub>5</sub>–O<sub>4'</sub> or the C<sub>5</sub>–N<sub>4'</sub> bond is more favorable kinetically than cleavage in the reverse order. We also found that the Dewar valence isomer can be reversed to the (6–4) product by both radical anion and radical cation pathways, though the anionic pathway has a much lower barrier. These calculations are in accord with the observation that the Dewar valence isomer is also reversed to the parent nucleotides by (6–4) photolyase, though much less efficiently than the (6–4) products.

## Introduction

UV irradiation of dipyrимidine sites in DNA produces two major direct photoproducts, the *cis,syn* cyclobutane pyrimidine dimers (CPD) **1** and the pyrimidine (6–4)pyrimidone ((6–4)) products **5**, the latter of which can be photoisomerized to their Dewar valence isomers **6** upon irradiation by UVB/A<sup>1,2</sup> (Figures 1 and 2). These lesions have been implicated in cell lethality, mutagenesis, and carcinogenesis.<sup>3,4</sup> To cope with these types of photodamage, organisms have developed a number of methods for their repair, the most fascinating of which is photoreactivation, which involves light-mediated reversal by enzymes known as photolyases.<sup>5</sup> The first of these enzymes to be discovered was the *cis,syn* CPD photolyase,<sup>6</sup> for which much evidence exists to suggest that they repair dimers by a visible light-induced electron transfer from a deprotonated dihydro flavin adenine dinucleotide cofactor (FADH<sup>–</sup>) to the substrate (Figure 1).<sup>5,7,8</sup> Many years later evidence was obtained that there also existed an enzyme that could photoreverse (6–4) products.<sup>9</sup>

\* To whom correspondence should be addressed. Phone: (314) 935-6721. Fax: (314) 935-4481. E-mail: taylor@wuchem.wustl.edu.

(1) Wang, S. Y. *Photochemistry and Photobiology of Nucleic Acids. Volume I: Chemistry*; Academic Press: San Diego, CA, 1976.

(2) Cadet, J.; Vigny, P. In *The photochemistry of nucleic acids*; Morrison, H., Ed.; John Wiley & Sons: New York, 1990; Vol. 1, pp 1–272.

(3) Sage, E. *Photochem. Photobiol.* **1993**, *57*, 163–174.

(4) Pfeifer, G. P. *Photochem. Photobiol.* **1997**, *65*, 270–283.

(5) Sancar, A. *Biochemistry* **1994**, *33*, 2–9.

(6) Rupert, C. S.; Goodgal, S. H.; Herriott, R. M. *J. Gen. Physiol.* **1958**, *41*, 451.

(7) Kim, S.-T.; Sancar, A. *Photochem. Photobiol.* **1993**, *57*, 895–904.

Enzymatic assays<sup>10</sup> and enzymatic digestion/HPLC analysis<sup>11</sup> showed that the (6–4) products are restored to the parental nucleotides by (6–4) photolyases. This was quite surprising at the time, as there was no obvious mechanism by which (6–4) products could be directly reversed by photoinduced electron transfer. Unlike the reversal of a CPD, which requires only breaking two bonds, reversal of a (6–4) product requires breaking the C<sub>6</sub>–C<sub>4'</sub> bond and transferring the –OH or –NH<sub>2</sub> group on C<sub>5</sub> of one nucleotide to C<sub>4'</sub> of the other nucleotide.

A mechanistic connection between CPD and (6–4) product repair could be made, however, if the (6–4) product was first enzymatically converted to a similar four-membered ring oxetane or azetidine substrate **7** (Figure 2), as one of us has suggested.<sup>10,12</sup> By analogy to CPD photolyase, it was then proposed that an electron is transferred from an electronically excited FADH<sup>–</sup> cofactor to the oxetane or azetidine **7** to give the anion radical intermediate **8**. The anion radical intermediate **8** would then undergo either a concerted or a stepwise fragmentation to give the radical anion **9** of the parental dinucleotide. The catalytic cycle is completed when the electron is transferred

(8) Park, H.-W.; Kim, S.-T.; Sancar, A.; Deisenhofer, J. *Science* **1995**, *268*, 1866–1872.

(9) Todo, T.; Takemori, H.; Ryo, H.; Ihara, M.; Matsunaga, T.; Nikaido, O.; Sato, K.; Nomura, T. *Nature* **1993**, *361*, 371–374.

(10) Kim, S. T.; Malhotra, K.; Smith, C. A.; Taylor, J. S.; Sancar, A. *J. Biol. Chem.* **1994**, *269*, 8535–8540.

(11) Hitomi, K.; Kim, S. T.; Iwai, S.; Harima, N.; Otsoshi, E.; Ikenaga, M.; Todo, T. *J. Biol. Chem.* **1997**, *272*, 32591–32598.

(12) Zhao, X.; Liu, J.; Hus, D. S.; Zhao, S.; Taylor, J.-S.; Sancar, A. *J. Biol. Chem.* **1997**, *272*, 32580–32590.

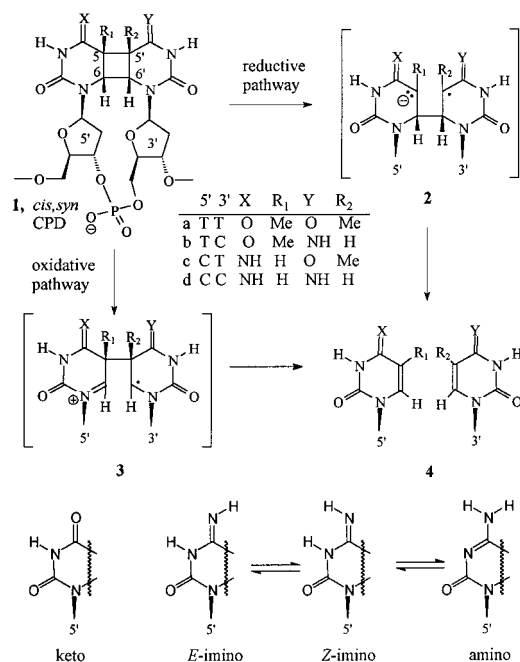


**Figure 1.** Structures of the *cis,syn* cyclobutane pyrimidine dimer (CPD) photoproducts and the intermediate involved in reductive and oxidative pathways for their reversal to the parental pyrimidines. Though thymine and thymine in dimers prefer the keto tautomer, cytosine prefers the amino tautomer and cytosine in dimers can adopt either amino or imino tautomeric forms (shown below). For convenience, however, cytosine and cytosine in the dimers and intermediates in the reaction scheme are shown only as their imino tautomers.

back from **9** to the FADH<sup>o</sup> to give the parental dinucleotide **4**. The thermodynamics of this pathway is diagrammed in Figure 3. In support of such a pathway, it has been shown that the oxetane **10**, formed by a Paterno–Buchi photocyclization reaction between **11** and **12**, can be reversed by both reductive and oxidative photoinduced electron-transfer mechanisms (Figure 2).<sup>13</sup> It has also been shown that the thio analogue of the (6-4) product **5e** can be photoreversed with 254-nm light, in a process involving the thietane intermediate **7e**, the sulfur analogue of an oxetane (Figure 2).<sup>14,15</sup> Evidence for a common mechanism for repair of CPDs and (6-4) products also comes from analysis of the protein sequences for (6-4) photolyases, which have a high degree of identity to those of the CPD photolyases.<sup>16–18</sup> Most recently, the recombinant (6-4) photolyases from *Drosophila melanogaster* and *Xenopus laevis* have been overexpressed and purified, and evidence for the existence of a reduced flavin intermediate has been obtained.<sup>11,12,17,19</sup>

Photoinduced reversal of CPDs has been recently investigated by semiempirical AM1 calculations, which suggest that the fragmentation of both radical anion and radical cation intermediates proceeds via a stepwise process by pathways shown in

(13) Prakash, G.; Falvey, D. E. *J. Am. Chem. Soc.* **1995**, *117*, 11375–11376.

(14) Clivio, P.; Fourrey, J.-L. *J. Chem. Soc., Chem. Commun.* **1996**, 2203–2204.

(15) Liu, J.; Taylor, J.-S. *J. Am. Chem. Soc.* **1996**, *118*, 3287–3288.

(16) Kanai, S.; Kikuno, R.; Toh, H.; Ryo, H.; Todo, T. *J. Mol. Evol.* **1997**, *45*, 535–548.

(17) Nakajima, S.; Sugiyama, M.; Iwai, S.; Hitomi, K.; Otoshi, E.; Kim, S. T.; Jiang, C. Z.; Todo, T.; Britt, A. B.; Yamamoto, K. *Nucleic Acids Res.* **1998**, *26*, 638–644.

(18) Todo, T.; Ryo, H.; Yamamoto, K.; Inui, T.; Ayaki, H.; Nomura, T.; Ikenaga, M. *Science* **1996**, *272*, 109–112.

(19) Todo, T.; Kim, S. T.; Hitomi, K.; Otoshi, E.; Inui, T.; Morioka, H.; Kobayashi, H.; Ohtsuka, E.; Toh, H.; Ikenaga, M. *Nucleic Acids Res.* **1997**, *25*, 764–768.

Figure 1.<sup>20</sup> Herein, we report semiempirical PM3 and AM1 calculations to locate the transition states in the fragmentation of neutral, radical anions, and radical cations of the proposed oxetane and azetidine intermediates involved in the photoenzymatic repair of (6-4) products. Our study suggests that, in the gas phase, the anion radical pathway is more favorable kinetically than the cation radical pathway. We also show that the Dewar product can be reversed to the (6-4) product via anion and cation radical intermediates, and though the barrier for splitting of the radical anion is much lower than for the radical cation, it is still higher than that calculated for the splitting of the anion radical of the oxetane intermediates. This latter result is in accord with the observation that Dewar photoproducts are also reversed by (6-4) photolyase, though much less efficiently.<sup>12</sup>

## Methods

Quantum calculations were carried out on a Silicon Graphics INDY R5000 workstation with Spartan 4.0 or 5.0.1 (Wavefunction, Inc., Irvine, CA). The geometries of the anion and cation radicals of the starting materials, intermediates, and product complexes were optimized at the semiempirical AM1<sup>21</sup> and PM3<sup>22</sup> levels. Calculations on open-shell species were carried out at the unrestricted Hartree–Fock level, and transition-state structures were found by using geometries obtained with the reaction coordinate method or by using the linear synchronous transit method. The location of a transition state was verified by numerical frequency analysis. Each transition state had only one imaginary frequency, and the normal mode associated with that frequency indicated that the transition state was on the correct reaction path. Molecular entropies were calculated using unscaled frequencies and standard statistical thermodynamics formulas.<sup>23</sup> Free energy changes at the standard temperature ( $T = 298.15$  K) were estimated as  $\Delta G = \Delta H - T\Delta S$ . Adiabatic electron affinities were calculated as the difference in heats of formation between the optimized structures for the anion and neutral, and adiabatic ionization potentials as the difference in the heats of formation between optimized cation and neutral. Vertical electron affinities were calculated as the difference between the heats of formation of the optimized neutral structure and the radical anion using the optimized structure of the neutral. Vertical ionization potentials were calculated in an analogous fashion. The electron affinities and ionization potentials were also calculated as the LUMO and HOMO energies according to Koopmans theorem. Spin and charge densities were obtained by natural population analysis.<sup>24</sup>

## Results and Discussion

### Selection of the Model Systems and Calculation Methods.

To simplify the calculations and to focus on the fundamental chemistry involved in the splitting of the oxetane and azetidine isomers of the (6-4) products, we chose to first study only the base portions of the photoproducts. The sugar phosphate backbone was not expected to significantly influence the geometry of the early steps in the splitting reaction but would be expected, along with the active site of the enzyme, to influence later stages by restricting the geometry of intermediates and product complexes. We chose Thy[ox]Thy (**13a**) and the two stereoisomers (*E* and *Z*) of Thy[az]Cyt (**13b**) as representatives of the oxetane and azetidine classes of photoproducts for detailed investigation of the splitting pathways (Figures 4a and 5a,b) by the two pathways shown in Figure 6a. To study the

(20) Voityuk, A. A.; Michel-Beyerle, M.-E.; Rosch, N. *J. Am. Chem. Soc.* **1996**, *118*, 9750–9758.

(21) Dewar, M. J. S.; Zoebisch, E. G.; Healy, E. F.; Stewart, J. J. P. *J. Am. Chem. Soc.* **1985**, *107*, 3902–3909.

(22) Stewart, J. J. P. *J. Comput. Chem.* **1989**, *10*, 209–220.

(23) Moore, W. J. *Physical Chemistry*, 4th ed.; Prentice Hall International, Inc.: London, 1972.

(24) Reed, A. E.; Weinstock, R. B.; Weinhold, F. *J. Chem. Phys.* **1985**, *83*, 735–746.

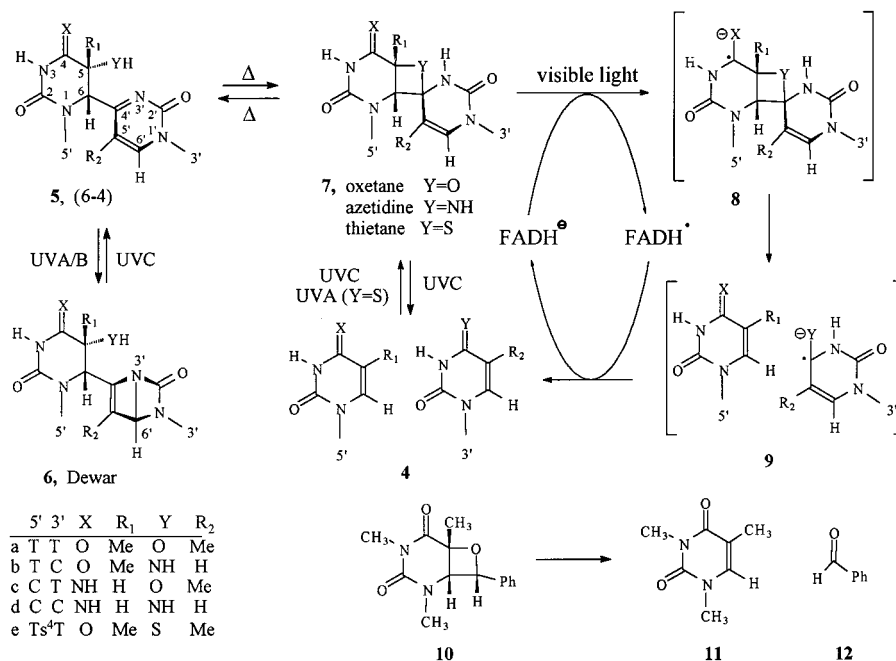


**Figure 2.** Proposed mechanism of the formation of (6–4) photoproducts by UV light and their reversal by (6–4) photolyase. Wavelength ranges are defined as UVA (320–360 nm), UVB (280–320 nm), and UVC (240–280 nm). For convenience, cytosine and cytosine in the 5' position of the photoproducts and intermediates are shown in their imino tautomeric form. See Figure 1 for the various tautomeric forms of C.

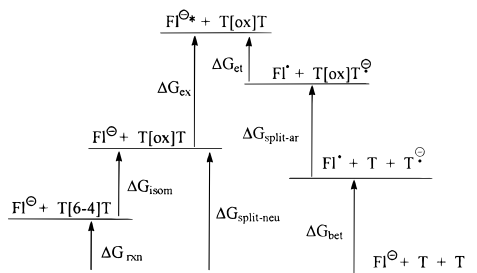


**Figure 3.** General thermodynamic scheme for the proposed pathway for reversal of the (6–4) photoproduct of TT by a photoinduced anion radical pathway (not to scale). Abbreviations used: FI, flavin; rxn, reaction; isom, isomerization; neu, neutral; ex, excitation; et, electron transfer; split, splitting; ar, anion radical; bet, back electron transfer.

effect of a cytosine in place of thymine on the splitting reaction, the amino and *E*-imino tautomers of Cyt[ox]Thy were also studied (Figure 4b,c). The imino tautomer was investigated because, whereas cytosine prefers the amino tautomer, cytosine in which the 5,6 double bond is saturated is known to adopt either amino or imino tautomeric forms, depending on the solvent.<sup>25</sup> In contrast, thymine is known to prefer the keto tautomer, both as the parent base and as part of *cis,syn* or (6–4) products.<sup>26,27</sup> The Dewar valence isomer of 1,4-dimethylpyrimid-2-one (15) was used as a model to study the reversal of the Dewar products to the (6–4) products (Figure 6b).

We initially chose to use semiempirical methods to study the splitting reactions because of the size of the substrates and the number of substrates and pathways to be explored, and the expectation that these methods would give reasonably accurate results for the system under study. In the latter regard, it has been found that activation barriers for splitting of the *cis,syn* cyclobutane uracil dimers determined by AM1<sup>20</sup> are in good

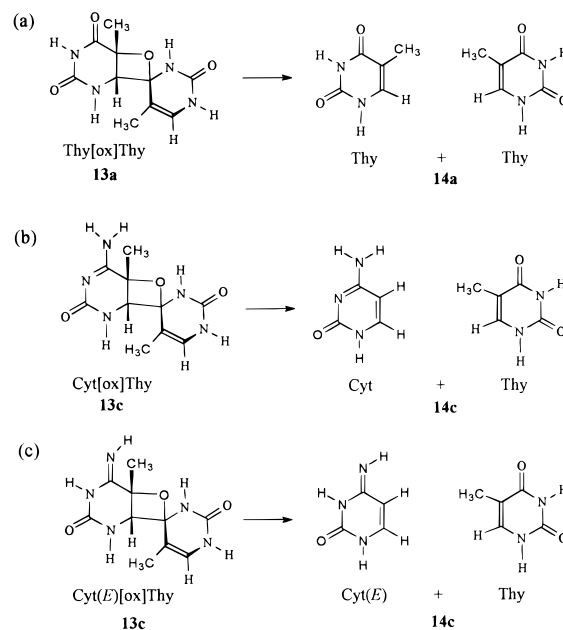


**Figure 4.** Structures of model systems used to study the splitting of the oxetane isomers.

agreement with subsequent calculations carried out by HF, MP2, and density functional methods. For the anion radical pathway, UHF calculations at the 6-31G\* level gave the first activation barrier as 6.2 kcal/mol, which dropped to –1.1 at the MP2 level.<sup>28</sup> It was estimated, however, that MP2 overcorrected the HF calculation and that the barrier would be more reasonably estimated as being less than 3 kcal/mol. These values compare quite favorably to that of 3.9 kcal/mol calculated by AM1. For the cation radical pathway, UHF/6-31G\*, MP2/6-31G\*, and B3LYP/6-31G\* all calculate a very low value (0.02–0.88 kcal/mol) for the first activation barrier in the splitting of the cation radical pathway, or none at all at the SCRFF/B3LYP/6-31G\*

(25) Brown, D. M.; Hewlins, M. J. E. *J. Chem. Soc. C* **1968**, 2050–2055.

(26) Cadet, J.; Voituriez, F. E.; Hruska, F. E.; Grand, A. *Biopolymers* **1985**, *24*, 897–903.

(27) Karle, I. L. *Acta Crystallogr.* **1969**, *B25*, 2119–2126.

(28) Voityuk, A. A.; Roesch, N. *J. Phys. Chem. A* **1997**, *101*, 8335–8338.

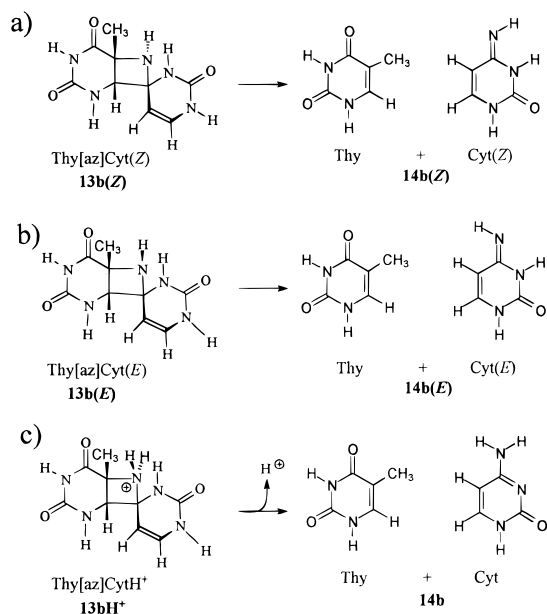


**Figure 5.** Structures of model systems used to study the splitting of the azetidine isomers.

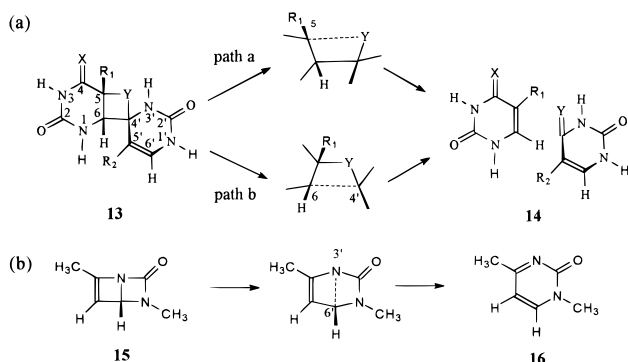


**Figure 6.** Bond-breaking pathways studied for (a) the splitting of the proposed oxetane and azetidine intermediates in the photoenzymatic reversal of (6-4) products and (b) the photoenzymatic conversion of the Dewar product to the (6-4) product.

level.<sup>29</sup> These results are in agreement with the activationless barrier calculated by AM1.

We also decided to carry out semiempirical calculations with PM3, because it has been shown to be better at predicting the experimental heats of formation for a number of compounds.<sup>30</sup> The average differences between calculated and experimental heats of formation for 657 normal-valent compounds and for 106 hypervalent compounds were (in kcal/mol) as follow: PM3, 7.8 and 13.6; AM1, 12.7 and 83.1; MNDO, 13.9 and 75.8.<sup>30</sup> Average errors for ionization potentials, bond angles, and dipole moments were found to be intermediate between those for MNDO and AM1, while errors on bond lengths are slightly reduced. PM3 also appears to be better in some cases in predicting activation barriers. For example, the barrier for the rearrangement of an addition complex of ethylene radical cation and ethylene to give 1-butene radical cation was calculated to be 6.1 kcal/mol by PMP4 (Møller–Plesset theory up to fourth order)/6-31G\*\*//MP2/6-31G\*\*, compared with 3.5 kcal/mol calculated by PM3 and 12.5 kcal/mol calculated by AM1.<sup>31</sup> The

structures of the transition state obtained by MP2/6-31G\*\* and by semiempirical methods are also similar. Comparisons between AM1, PM3, and ab initio calculations have also been made for a number of other systems.<sup>32–36</sup>

**Thermodynamics of Isomerization and Splitting.** The gas-phase heats of formation and the molecular entropies for the neutral, anion, and cation radical of the thymine, cytosine and its two imino tautomers, Thy[6-4]Thy, Thy[6-4]Cyt, Thy[ox]-Thy, and the two isomers for Thy[az]Cyt were calculated (Table 1). The AM1 energy of Thy[ox]Thy is higher than that of Thy[6-4]Thy by 19.0 kcal/mol, compared to 8.6 kcal/mol calculated by PM3, which is quite close to the 9–11 kcal/mol estimated by nonlocal density functional theory.<sup>37</sup> Experimentally, the presumed oxetane photoproduct of thymine has been shown to be unstable above  $-80$  °C and thermally decomposes to the (6-4) product.<sup>38</sup> The analogous thietane (Figure 2, Y = S), however, has been shown to slowly interconvert with the (6-4) product and gives a 3:1 mixture in water at room temperature.<sup>39</sup> Whereas AM1 calculates the enthalpy difference between the thietane and (6-4) isomer to be  $-5$  kcal/mol,<sup>37</sup> PM3 calculates the difference to be 2.6 kcal/mol, which is more in accord with the experimental data. Surprisingly, PM3 predicts the isomerization of Thy[6-4]Cyt to either isomer of Thy[az]-Cyt to be exothermic ( $-0.3$  to  $-4.4$  kcal/mol), in contrast to the isomerization of Thy[6-4]Thy to Thy[ox]Thy, which it predicts to be endothermic (8.6 kcal/mol). AM1 calculates the isomerization to the azetidine isomers as being endothermic (12.9 and 14.7 kcal/mol), though less than for isomerization to the oxetane isomer (19.0 kcal/mol). There is no evidence from NMR, however, that the (6-4) photoproduct of the dinucleotide TpdC is in appreciable equilibrium with the azetidine form.<sup>40,41</sup>

From the data in Table 2, it can be seen that the enthalpy changes calculated by AM1 for the splitting of Thy[ox]Thy and Thy[az]Cyt(Z) are  $-28.9$  and  $-14.3$  kcal/mol, respectively, compared to  $-18.6$  and  $-1.3$  kcal/mol calculated by PM3. For comparison, the enthalpy change for the splitting of oxetane ( $C_3H_6O$ ) into ethene and formaldehyde is calculated by AM1 and PM3 to be 10.5 and 9.3 kcal/mol, respectively, while the value based on the experimental heats of formation<sup>42</sup> is 4.09 kcal/mol. There is no experimental value for the thermolysis of azetidine to ethene and methyleneimine, but ab initio studies at the 3-21G level predict that it is an endothermic reaction,<sup>43</sup> and AM1 and PM3 give  $\Delta H = 14.0$  and 28.3 kcal/mol, respectively. The exothermic nature of the splitting of Thy[ox]-Thy and Thy[az]Cyt(Z) in comparison to the endothermic splitting of the parent oxetane and azetidine can be attributed to the effect of the ring substituents. The same change from

(32) Mulholland, A. J.; Richards, W. G. *Int. J. Quantum Chem.* **1994**, *51*, 161–172.

(33) Andres, J.; Domingo, L. R.; Picher, M. T.; Safont, V. S. *Int. J. Quantum Chem.* **1998**, *66*, 9–24.

(34) Anh, N. T.; Frison, G.; Sollandi-Cavallo, A.; Metzner, P. *Tetraedron* **1998**, *54*, 12841–12852.

(35) Jursic, B. S.; Zdravkovski, Z. *Theochem* **1994**, *115*, 249–257.

(36) Morpurgo, S.; Bossa, M.; Morpurgo, G. O. *Theochem* **1998**, *429*, 71–80.

(37) Heelis, P. F.; Liu, S. *J. Am. Chem. Soc.* **1997**, *119*, 2936–2937.

(38) Rahn, R. O.; Hosszu, J. L. *Photochem. Photobiol.* **1969**, *10*, 131–137.

(39) Clivio, P.; Fourrey, J.-L.; Gasche, J.; Favre, A. *J. Am. Chem. Soc.* **1991**, *113*, 5481–5483.

(40) Taylor, J.-S.; Lu, H.-F.; Kotyk, J. J. *Photochem. Photobiol.* **1990**, *51*, 161–167.

(41) Franklin, W. A.; Doetsch, P. W.; Haseltine, W. A. *Nucleic Acids Res.* **1985**, *13*, 5317–5325.

(42) Afeefy, H. Y.; Liebman, J. F.; Stein, S. E. In *Neutral Thermochemical Data*; Mallard, W. G., Linstrom, P. J., Eds.; National Institute of Standards and Technology: Gaithersburg MD, 1998.

(43) Chen, G.; Fu, X.; Tang, A. *Chin. J. Chem.* **1992**, *10*, 193–199.

(29) Rak, J.; Voityuk, A. A.; Roesch, N. *J. Phys. Chem. A* **1998**, *102*, 7168–7175.

(30) Stewart, J. J. P. *J. Comput. Chem.* **1989**, *10*, 221–264.

(31) Alvarez-Idaboy, J. R.; Eriksson, L. A.; Fangstrom, T.; Lunell, S. *J. Phys. Chem.* **1993**, *97*, 12737–12741.

**Table 1.** Calculated Gas-Phase Heats of Formation and Molecular Entropies for the Proposed Intermediates Involved in the Thermal and Electron-Transfer-Catalyzed Reversal of the (6-4) Photoproducts of Thymine and Cytosine

molecule	heats of formation (kcal mol <sup>-1</sup> )						molecular entropy (cal mol <sup>-1</sup> K <sup>-1</sup> )					
	neutral		anion		cation		neutral		anion		cation	
	AM1	PM3	AM1	PM3	AM1	PM3	AM1	PM3	AM1	PM3	AM1	PM3
Thy	-61.0	-75.8	-87.0	-104.4	140.0	123.8	84.5	85.6	91.3	85.9	88.8	85.6
Cyt	2.7	-13.9	-24.6	-46.6	201.2	181.9	81.1	82.2	84.1	83.0	81.4	82.9
Cyt(Z)	4.2	-8.1	-14.7	-31.1	198.2	182.7	80.9	78.8	80.8	81.3	79.9	82.6
Cyt(E)	6.2	-10.7	-14.4	-35.3	201.0	180.5	81.1	78.0	81.0	80.5	80.0	81.6
Thy[6-4]Thy	-112.1	-141.6	-159.0	-193.9	-84.8	57.3	126.9	132.6	128.3	130.5	128.1	131.0
Thy[ox]Thy	-93.1	-133.0	-112.9	-158.8	99.4	61.5	126.9	129.6	125.6	116.3	128.8	129.0
Thy[6-4]Cyt	-58.7	-88.1	-105.0	-139.4	145.1	118.3	121.3	127.6	121.4	123.9	120.0	125.4
Thy[az]Cyt(Z)	-44.0	-88.4	-64.0	-113.3	150.6	106.2	121.3	124.0	121.8	123.2	122.0	124.6
Thy[az]Cyt(E)	-45.8	-92.5	-66.8	-117.9	105.9 <sup>a</sup>	106.5	119.1	122.9	120.4	123.7	125.2 <sup>a</sup>	123.6

<sup>a</sup> Energy of the intermediate.**Table 2.** Enthalpy and Free Energy Changes for the Gas-Phase Reversal of the (6-4) Photoproducts and Oxetane and Azetidine Isomers to Fully Dissociated Products, Calculated by AM1 and PM3<sup>a</sup>

reaction	$\Delta H$ (kcal/mol)		$\Delta G$ (kcal/mol)	
	AM1	PM3	AM1	PM3
Thy[6-4]Thy $\rightarrow$ 2 Thy	-9.9	-10.0	-22.5	-21.5
Thy[ox]Thy $\rightarrow$ 2 Thy	-28.9	-18.6	-41.4	-31.0
Thy[ox]Thy <sup>-</sup> $\rightarrow$ Thy + Thy <sup>-</sup>	-35.1	-21.4	-50.1	-37.9
Thy[ox]Thy <sup>+</sup> $\rightarrow$ Thy + Thy <sup>+</sup>	-20.4	-13.5	-33.7	-26.1
Cyt[ox]Thy <sup>-</sup> $\rightarrow$ Cyt <sup>-</sup> + Thy	nd	-19.4	nd	-31.9
Cyt(E)[ox]Thy <sup>-</sup> $\rightarrow$ Cyt(E) + Thy <sup>-</sup>	nd	-22.3 (-29.6)	nd	-37.5 (-41.7)
Thy[6-4]Cyt $\rightarrow$ Thy + Cyt	0.4	-1.6	-12.8	-13.6
Thy[az]Cyt(Z) $\rightarrow$ Thy + Cyt(Z)	-12.8 (-14.3)	4.5 (-1.3)	-25.9 (-27.5)	-7.5 (-14.4)
Thy[az]Cyt(Z) <sup>-</sup> $\rightarrow$ Thy <sup>-</sup> + Cyt(Z)	-18.8 (-21.6)	0.8 (-9.1)	-33.8 (-35.6)	-11.6 (-22.6)
Thy[az]Cyt(Z) <sup>+</sup> $\rightarrow$ Thy + Cyt(Z) <sup>+</sup>	-13.4 (-10.4)	0.7 (-0.1)	-26.0 (-23.5)	-12.3 (-13.2)
Thy[az]Cyt(E) $\rightarrow$ Thy + Cyt(E)	-9.0 (-12.5)	6.0 (2.8)	-22.9 (-26.4)	-6.1 (-10.6)
Thy[az]Cyt(E) <sup>-</sup> $\rightarrow$ Thy <sup>-</sup> + Cyt(E)	-14.0 (-18.8)	2.8 (-4.5)	-29.5 (-33.2)	-9.2 (-17.9)
Thy[az]Cyt(E) <sup>+</sup> $\rightarrow$ Thy + Cyt(E) <sup>+</sup>	39.3 (34.3) <sup>b</sup>	-1.8 (-0.4)	22.4 (22.2) <sup>b</sup>	-14.8 (-13.8)

<sup>a</sup> Values in parentheses are for conversion to the more stable amino tautomer, Cyt. In the case of the radical anion decompositions, the value is for conversion to Thy + Cyt<sup>-</sup>. <sup>b</sup> Values for the intermediate to the product complex; see note *a* in Table 1.

endothermic to exothermic is predicted to occur when the parent oxetane is substituted with methyl groups.

As is the case for *cis,syn* dimers,<sup>20</sup> transferring an electron to or from the oxetane and azetidine intermediates changes the  $\Delta H$  and  $\Delta G$  of the splitting reactions. Transferring an electron to the Thy[ox]Thy intermediate changes the  $\Delta H$  of splitting from -28.9 to -35.1 kcal/mol and  $\Delta G$  from -41.4 to -50.1 kcal/mol, as calculated by the AM1 method (Table 2). The same trend is observed for the reversal of both isomers of Thy[az]-Cyt, and PM3 gives similar results. In contrast, abstracting an electron from the oxetane substrate increases both the  $\Delta H$  and  $\Delta G$  for the dimer splitting relative to those of the neutral oxetane and decreases both  $\Delta H$  and  $\Delta G$  for splitting of both azetidine isomers, as calculated by either AM1 or PM3. It should be noted that the C<sub>6</sub>-C<sub>4'</sub> bond is broken during geometry optimization of the *E* stereoisomer by AM1. The entropy terms contribute about 10-20 kcal/mol to the free energy changes in these gas-phase reactions at room temperature. The entropy term may not contribute as much to the free energy in the enzymatic process due to binding of the product pyrimidines by the enzyme and by the DNA backbone.

**Splitting Pathways.** The radical anion or cation of the oxetane or azetidine intermediate can follow a concerted pathway in which C<sub>5</sub>-Y and C<sub>6</sub>-C<sub>4'</sub> bonds break simultaneously, or a stepwise pathway in which either bond breaks first (Figure 6a). When the C<sub>5</sub>-O<sub>4'</sub> bond in Thy[ox]Thy anion radical was stretched from the equilibrium bond length in the starting material to 3.0 Å, the length of the C<sub>6</sub>-C<sub>4'</sub> bond remained relatively constant. Similarly, when the C<sub>6</sub>-C<sub>4'</sub> bond in the cation radical of Thy[ox]Thy was stretched, the length of the C<sub>5</sub>-O<sub>4'</sub> bond did not change very much, either. The same

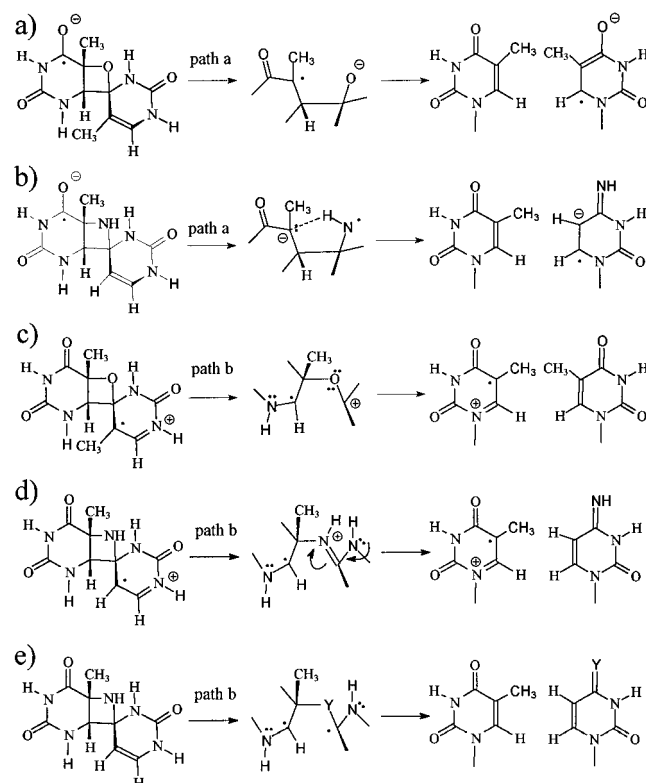
behavior was observed for both stereoisomers of Thy[az]Cyt in both anion and cation radical pathways, indicating that the lowest energy pathway for splitting occurs via a stepwise process and not by a concerted pathway in the gas phase. The failure to detect a concerted pathway may also have to do with the fact that AM1 and PM3 methods tend to predict stepwise rather than concerted reaction pathways for cycloaddition reactions such as the Diels-Alder reaction because of the neglect of orbital overlap.<sup>34</sup> It is not unreasonable, however, to expect that the lowest energy pathway in the splitting of oxetanes and azetidines occurs by a stepwise mechanism due to the presence of a heteroatom.

To determine which stepwise bond cleavage pathway is more favorable, the transition-state calculations were carried out with both AM1 and PM3 levels for each pathway. Whereas transition states could always be located by PM3, it was found that AM1 generally could not locate transition states for path b in the anion radical pathway and for path a in the cation radical pathway. The relative energies of the stationary points found are given in Table 3 and diagrammed in Figure 8. As can be seen, the splitting reactions are more exothermic than calculated from the heats of formation of the individual products (Table 2) due to formation of stabilized product complexes. Whereas cleavage pathway a was kinetically favored for the anion radicals over path b, which had a high second barrier, the neutral and cation radical intermediates favored path b over path a, which had a high first barrier. The lack of a clear preference for breaking either the C<sub>5</sub>-O<sub>4'</sub> or the C<sub>6</sub>-C<sub>4'</sub> bond as a first step in splitting of the anion radical of the oxetane or the azetidine was unexpected, as it was thought that the intermediate in path a would be better able to stabilize a negative charge (Figure 7a,b).

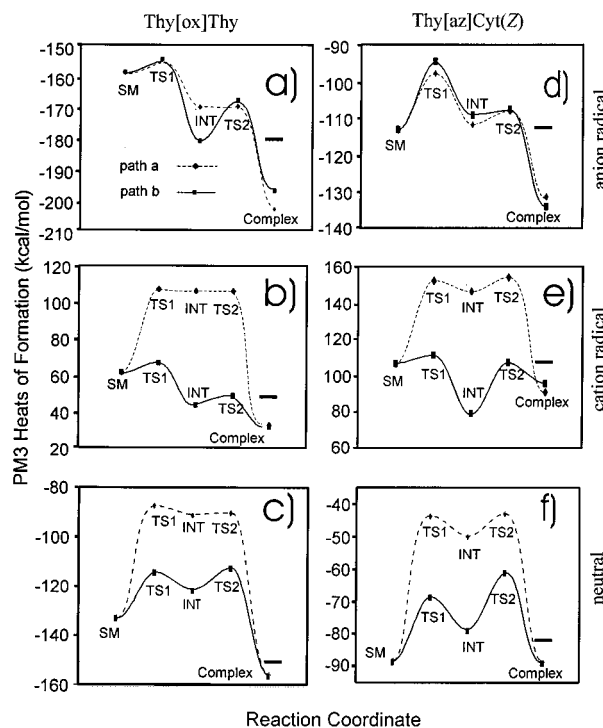
**Table 3.** Relative Energies (kcal/mol) of the Stationary Points<sup>a</sup> in the Gas-Phase Fragmentation of the Radical Cations and Anions of Oxetane and Azetidine Isomers of (6-4) Products of Thymine and Cytosine Calculated by PM3 and AM1 (AM1 Data in Parentheses)

dimer	path	TS1 = $\Delta H^{\ddagger 1}$	int	TS2	$\Delta H^{\ddagger 2}$	complex
Thy[ox]Thy	a	45.4	41.8	42.7	0.9	-23.3
	b	19.0	11.4	20.6	9.2	-23.3
Thy[ox]Thy <sup>-</sup>	a	4.2 (3.6)	-11.3 (-22.6)	-11.0 (-21.6)	0.3 (1.0)	-44.3 (-43.4)
	b	4.1	-22.5	-9.2	13.3	-38.4
Thy[ox]Thy <sup>+</sup>	a	45.7	44.3	44.6	0.3	-29.0
	b	5.0 (1.7)	-17.8 (-31.1)	-13.1 (-26.3)	4.7 (4.8)	-30.1 (-33.8)
Thy[az]Cyt(Z)	a	45.0	38.6	45.6	7.0	-0.5
	b	20.1	9.8	27.6	17.8	-0.5
Thy[az]Cyt(Z) <sup>-</sup>	a	15.4 (16.8)	1.4 (-3.5)	5.2 (-2.7)	3.8 (0.8)	-18.3 (-29.0)
	b	18.8	4.0	5.8	1.8	-20.8
Thy[az]Cyt(Z) <sup>+</sup>	a	45.8	40.1	47.6	7.5	-15.3
	b	5.0 (0.0)	-27.5 (-39.6)	1.0 (-12.2)	28.5 (27.4)	-11.2 (-19.3)
Thy[az]Cyt(E)	a	45.6	42.9	50.2	7.3	2.5
	b	20.7	12.4	16.8	4.4	2.5
Thy[az]Cyt(E) <sup>-</sup>	a	16.1 (19.3)	5.5 (-0.7)	9.5 (0.3)	4.0 (1.0)	-13.9 (-52.2)
	b	9.7	-20.7	4.7	25.4	-9.4
Thy[az]Cyt(E) <sup>+</sup>	a	47.1	40.0	46.8	6.8	-15.4
	b	2.1 (na <sup>b</sup> )	-29.1 (na)	0.0 (na)	29.1 (33.0)	-5.0 (na)
Cyt[ox]Thy <sup>-</sup>	a	7.4	-5.3	-4.3	1.0	-30.6
Cyt(E)[ox]Thy <sup>-</sup>	a	2.6	-16.5	-14.8	1.7	-38.6

<sup>a</sup> "TS1", "TS2", "int", and "complex" are the first and second transition states, intermediate, and product complex, respectively. The energies given are relative to the starting point of each pathway.  $\Delta H^{\ddagger 1}$  and  $\Delta H^{\ddagger 2}$  are the activation enthalpies for the two steps of cleavage. <sup>b</sup> Not available as the starting material fragmented on minimization.

**Figure 7.** Chemical representations of the intermediates involved in the fragmentations of the oxetane and azetidine intermediates by path a for the anion radicals (a,b) and by path b for the cation radicals (c,d) and the neutral (e) based on charge and spin density calculations.

In the splitting of the anion radical of the *cis,syn* dimers, breaking the C<sub>5</sub>-C<sub>5'</sub> bond followed by the C<sub>6</sub>-C<sub>6'</sub> bond (Figure 1)<sup>20</sup> was found to be much more favorable than breaking the bonds in the reverse order because of resonance stabilization of the anion in the intermediate **2** by the C<sub>4</sub> keto group (Figure 1). For the cation radicals of the oxetane and azetidine intermediates, the pathway in which the C<sub>6</sub>-C<sub>4'</sub> bond breaks first, followed by the breaking of the C<sub>5</sub>-O<sub>4'</sub> or the C<sub>5</sub>-N<sub>4'</sub> bond, is much more favorable than in the reverse order. This

**Figure 8.** Reaction coordinate diagrams for the fragmentation of (a) the anion radical of Thy[ox]Thy, (b) the cation radical of Thy[ox]Thy, (c) neutral Thy[ox]Thy, (d) the anion radical of Thy[az]Cyt(Z), (e) the cation radical of Thy[az]Cyt(Z), and (f) neutral Thy[az]Cyt(Z) by both path a (dashed line, breaking the C<sub>5</sub>-Y<sub>4'</sub> bond first) and path b (solid line, breaking the C<sub>6</sub>-C<sub>4'</sub> bond first) as calculated by PM3. The heats of formation for the fully dissociated products are shown by heavy bars.

again makes chemical sense (Figure 7c,d) and parallels the preferred bond cleavage pathway observed for splitting of the cation radical **3** of the *cis,syn* dimers (Figure 1).<sup>20</sup> The splitting of neutral oxetane and azetidine parallels the cation radical pathway and favors the pathway in which the C<sub>6</sub>-C<sub>4'</sub> bond breaks first (Table 3), probably due to the greater stabilization of the diradical by the two nitrogen centers (Figure 7e). It is important to note that an optimized geometry for the intermedi-

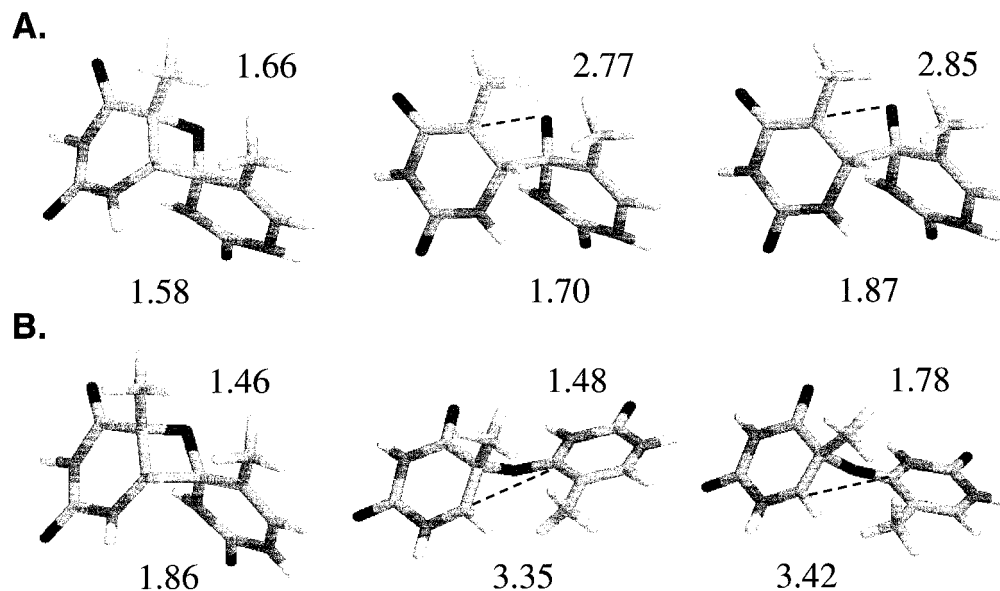


**Figure 9.** Structures of the first transition state, the intermediate, and the second transition state for the splitting of (a) the anion radical of Thy[ox]Thy through path a and (b) the cation radical of Thy[ox]Thy through path b. The length in angstroms of the  $C_5-O_4$  bond is shown above the structure, and that of the  $C_6-C_{4'}$  bond is shown below the structure.

ate in these cases could only be obtained by PM3 for the triplet state, as calculations on the singlet state led only back to the oxetane or forward to the free bases.

The energy barrier for splitting of the anion radical of Thy[az]Cyt by pathway a is much higher than that for Thy[ox]Thy, presumably because the  $C_{4'}$  nitrogen atom in the breaking bond is less able to stabilize a negative charge than is an oxygen. In support of this explanation, the negative charge is localized on the  $C_{4'}$  oxygen of the intermediate in the splitting of the oxetane by pathway a, and the spin is localized on the  $C_5$  carbon (Figure 7a). For the intermediate in the splitting of the azetidine by pathway a, the negative charge becomes localized on  $C_5$  and the spin on the  $C_{4'}$  nitrogen (Figure 7b). In addition, the hydrogen on the  $C_{4'}$  nitrogen points toward the negative charge at  $C_5$  and presumably helps stabilize the intermediate by hydrogen bonding. Whereas the gas-phase energy barriers for splitting of the anion radical of the oxetane and azetidine are different, the first barriers in splitting of the cation radical intermediates by path b are of about the same energy and quite low. This makes sense, because in pathway b a similarly substituted carbon-carbon bond is being broken in both the oxetane and the azetidine (Figure 7c,d). In contrast, the second barrier is much higher for the azetidine than for the oxetane, which is partly due to a more stabilized intermediate. Examination of the structures of the intermediates show that the two pyrimidine rings have reoriented themselves in such a way as to maximize conjugation of the nitrogen atom linking the two rings. A similar reorientation of the pyrimidine ring systems is seen in the intermediate for splitting of the cation radical of the oxetane intermediate (Figure 9). Such a reorientation would not be possible in DNA because of restrictions placed on the rings by the sugar phosphate backbone, and the intermediates in such a restricted system would be expected to be of higher energy. If so, the transition-state barriers for the second step in the reaction would also decrease, and this step might not be as rate-limiting as the unrestricted gas-phase calculations indicate.

**Electron Affinities and Ionization Potentials.** Another question that needs to be addressed is whether back electron transfer can occur in a stepwise splitting reaction via the two pathways. This can be determined by comparing the electron affinities and ionization potentials of the neutral intermediates

**Table 4.** Electron Affinities and Ionization Potentials for Species Involved in the Splitting of the Oxetane and Azetidine Isomers of the (6-4) Products as Calculated by PM3

	adiabatic		vertical		Koopmans theorem	
	EA (eV)	IP (eV)	EA (eV)	IP (eV)	EA (eV)	IP (eV)
Thy	-1.24	8.68	-0.98	8.91	-0.49	9.43
Cyt	-1.42	8.51	-1.03	8.71	-0.53	9.27
Cyt(Z)	-1.00	8.29	-0.72	8.54	-0.25	9.06
Cyt(E)	-0.28	8.31	-0.80	8.54	-0.32	9.06
Cyt[ox]Thy	-1.57	nd <sup>a</sup>	-1.09	nd	-0.54	nd
int, path a	-3.37	nd	-3.25	nd	-0.32	nd
Thy[ox]Thy	-1.12	8.46	-0.62	9.72	-0.32	9.53
int, path a	-3.50	8.50	-3.19	8.92	-0.36	9.62
int, path b	-2.56	7.13	-1.09	7.65	-0.03	8.29
Thy[az]Cyt(Z)	-1.08	8.46	-0.70	9.03	-0.23	9.60
int, path a	-2.70	8.52	-2.14	9.16	-0.32	9.74
int, path b	-1.33	6.84	-1.02	7.62	-0.05	8.23
Thy[az]Cyt(E)	-1.10	8.65	-0.46	9.58	-0.31	9.61
int, path a	-2.73	8.53	-1.80	9.31	-0.39	9.76
int, path b	-2.54	6.85	-0.56	8.19	-0.04	8.28

<sup>a</sup> Not determined.

with the precursor oxetanes and azetidines. Such calculations suggest that back electron transfer is unlikely to occur along the preferred pathways (Table 4). As one can see, the adiabatic electron affinities calculated by PM3 for Thy[ox]Thy and both stereoisomers of Thy[az]Cyt are approximately -1.10 eV, slightly less than those of -1.24 and -1.42 eV calculated for thymine and cytosine. There are no experimental electron affinities for DNA bases, but single-point calculations at the 6-31G\* level based on 3-21G geometries gave adiabatic electron affinities of -1.45 and -1.73 eV for thymine and cytosine.<sup>44</sup> The adiabatic ionization potentials for thymine, cytosine, Thy[ox]Thy, and both stereoisomers of Thy[az]Cyt calculated by PM3 are approximately 8.5 eV and within 0.21 eV of each other. The corresponding vertical ionization potentials based on the energy of the HOMOs calculated by PM3 (Koopmans theorem) are approximately 1 eV higher and only within 0.34 eV of each other. These values closely parallel the

(44) Colson, A.-O.; Besler, B.; Close, D. M.; Sevilla, M. D. *J. Phys. Chem.* **1992**, *96*, 661-668.

**Table 5.** PM3-Calculated Lengths (Å) of the Bonds Undergoing Cleavage in the Fragmentation Reactions by Path a or Path b

	Thy[ox]Thy <sup>-</sup>				Thy[ox]Thy <sup>+</sup>				Thy[ox]Thy			
	path a		path b		path a		path b		path a		path b	
	C <sub>5</sub> -O <sub>4'</sub>	C <sub>6</sub> -C <sub>4'</sub>	C <sub>5</sub> -O <sub>4'</sub>	C <sub>6</sub> -C <sub>4'</sub>	C <sub>5</sub> -O <sub>4'</sub>	C <sub>6</sub> -C <sub>4'</sub>	C <sub>5</sub> -O <sub>4</sub>	C <sub>6</sub> -C <sub>4'</sub>	C <sub>5</sub> -O <sub>4'</sub>	C <sub>6</sub> -C <sub>4'</sub>	C <sub>5</sub> -O <sub>4</sub>	C <sub>6</sub> -C <sub>4'</sub>
SM	1.440	1.611	1.440	1.611	1.472	1.601	1.472	1.601	1.465	1.593	1.465	1.593
TS1	1.663	1.583	1.466	2.294	2.285	1.604	1.459	1.862	2.232	1.597	1.453	2.107
int	2.770	1.701	1.443	2.996	2.352	1.611	1.479	3.356	3.019	1.594	1.448	2.802
TS2	2.848	1.869	1.755	3.061	2.682	1.747	1.781	3.425	2.699	1.732	1.736	2.919
complex	3.969	3.770	4.168	3.816	3.145	4.053	3.907	3.806	3.752	5.142	3.752	5.142
	Thy[az]Cyt(Z) <sup>-</sup>				Thy[az]Cyt(Z) <sup>+</sup>				Thy[az]Cyt(Z)			
	path a		path b		path a		path b		path a		path b	
	C <sub>5</sub> -N <sub>4'</sub>	C <sub>6</sub> -C <sub>4'</sub>	C <sub>5</sub> -N <sub>4'</sub>	C <sub>6</sub> -C <sub>4'</sub>	C <sub>5</sub> -N <sub>4'</sub>	C <sub>6</sub> -C <sub>4'</sub>	C <sub>5</sub> -N <sub>4'</sub>	C <sub>6</sub> -C <sub>4'</sub>	C <sub>5</sub> -N <sub>4'</sub>	C <sub>6</sub> -C <sub>4'</sub>	C <sub>5</sub> -N <sub>4'</sub>	C <sub>6</sub> -C <sub>4'</sub>
SM	1.523	1.580	1.523	1.580	1.516	1.601	1.516	1.601	1.517	1.586	1.517	1.586
TS1	2.195	1.579	1.514	2.096	2.237	1.596	1.509	1.855	2.223	1.583	1.507	2.109
int	2.922	1.617	1.517	3.002	3.021	1.596	1.520	3.089	3.084	1.583	1.506	2.948
TS2	3.131	1.944	2.082	3.221	3.091	1.978	2.340	3.616	3.798	1.925	1.926	3.099
complex	4.782	3.573	3.915	3.845	4.478	6.554	3.900	3.843	5.364	5.069	5.364	5.069
	Thy[az]Cyt(E) <sup>-</sup>				Thy[az]Cyt(E) <sup>+</sup>				Thy[az]Cyt(E)			
	path a		path b		path a		path b		path a		path b	
	C <sub>5</sub> -N <sub>4'</sub>	C <sub>6</sub> -C <sub>4'</sub>	C <sub>5</sub> -N <sub>4'</sub>	C <sub>6</sub> -C <sub>4'</sub>	C <sub>5</sub> -N <sub>4'</sub>	C <sub>6</sub> -C <sub>4'</sub>	C <sub>5</sub> -N <sub>4'</sub>	C <sub>6</sub> -C <sub>4'</sub>	C <sub>5</sub> -N <sub>4'</sub>	C <sub>6</sub> -C <sub>4'</sub>	C <sub>5</sub> -N <sub>4'</sub>	C <sub>6</sub> -C <sub>4'</sub>
SM	1.511	1.606	1.511	1.606	1.517	1.606	1.517	1.606	1.517	1.586	1.517	1.586
TS1	2.230	1.581	1.509	2.350	2.250	1.599	1.510	1.787	2.407	1.585	1.508	2.120
int	2.903	1.616	1.507	3.051	2.959	1.609	1.508	3.092	3.069	1.584	1.512	2.895
TS2	3.094	1.941	2.108	3.291	2.963	1.938	2.310	3.641	3.072	1.915	1.912	3.824
complex	4.697	3.563	4.786	3.730	4.977	6.583	3.655	3.912	4.570	4.146	4.570	4.146

experimental adiabatic ionization potentials for thymine and cytosine of 8.87 and 8.68 eV, respectively,<sup>45</sup> and the experimental vertical ionization potentials of 9.14 and 8.94 eV, respectively.<sup>46</sup> As one can see from Table 4, the adiabatic electron affinities for the neutral form of the intermediates involved in the radical anion splitting of Thy[ox]Thy or both isomers of Thy[az]Cyt in the kinetically preferred path a are greater than those of the precursor oxetane or azetidene. This would suggest that back electron transfer from the radical anion intermediates is unlikely to compete with back electron transfer from either the precursor or the product radical anions. Likewise, the adiabatic ionization potentials for the neutral form of the intermediates involved in the preferred path b for splitting of the radical cation, of Thy[ox]Thy and both isomers of Thy[az]Cyt are less than those for the precursor oxetane or azetidene. Again, this would suggest that back electron transfer to the intermediate radical cation is unlikely to compete with back electron transfer to the precursor radical cations.

**Geometries.** Though it is predicted by the calculations that transferring an electron to or from the dimer leads to appreciably different reactivities for Thy[ox]Thy and Thy[az]Cyt, it does not affect the bond lengths very much. For example, based on PM3 calculations, the bond lengths of C<sub>5</sub>-O<sub>4'</sub> and C<sub>6</sub>-C<sub>4'</sub> in the neutral Thy[ox]Thy are 1.47 and 1.59 Å, respectively, and change to 1.44 and 1.61 Å, respectively, in the anion radical and to 1.47 and 1.60 Å, respectively, in the cation radical. The changes in bond distances along the reaction pathways are given in Table 5. Whereas the bond length of C<sub>5</sub>-O<sub>4'</sub> in Thy[ox]Thy anion radical is calculated to increase by 0.22 Å on going to the first transition state along path a by PM3, the bond length of C<sub>5</sub>-N<sub>4'</sub> in the E and Z stereoisomers of Thy[az]Cyt increases by ~0.6 and ~0.7 Å, respectively. This difference in bond lengths is consistent with the low activation energy of 4.2 kcal/

mol for Thy[ox]Thy and the higher activation energies of 15.4 and 16.1 kcal/mol for the two isomers of Thy[az]Cyt (Table 3). On the other hand, the activation energies for path b of the radical cations of all the intermediates are similar and hence show similar small increases of about 0.2 Å in the C<sub>6</sub>-C<sub>4'</sub> bond lengths on reaching the transition state. The activation energies for path a of all the neutral intermediates are high (~45 kcal/mol, Table 3) and hence show similar large increases of about 0.6 ~ 0.9 Å in C<sub>5</sub>-Y bond lengths leading to the TS1. The transition-state structures for the splitting of Thy[ox]Thy in path a of the anion radical pathway and path b for the cation radical pathway are shown in Figure 9.

**Spin and Charge Densities.** For photoinduced DNA repair, it is important to rationalize the chemical reactivity and its dependence on the electronic structures of individual species involved in the processes of dimer splitting. It is particularly important to understand why the sequences of bond cleavages are different in anion radical and cation radical pathways. To gain further insight into the mechanism, the charge distributions along all reaction paths were determined by natural population analysis.<sup>24</sup> The total charge on the 5'- and 3'-bases along the reaction paths shows that the charge is more delocalized in the transition states than in the starting materials, intermediates, and product complexes (Table 6).

Addition of an electron to Thy[ox]Thy introduces an unpaired electron and a negative charge on the 5'-pyrimidine of the photoproduct (see Figure 7a). The calculated spin densities are  $\rho(C_4) = 0.54$  and  $\rho(O_4) = 0.28$ . The unpaired electron on C<sub>4</sub> is thus in a position to form a  $\pi$  bond with C<sub>5</sub> with the concomitant cleavage of the C<sub>5</sub>-O<sub>4'</sub> bond. In the intermediate, the unpaired electron is centered on C<sub>5</sub> ( $\rho(C_5) = 0.89$ ) which is in a position to form a  $\pi$  bond with C<sub>6</sub> with the concomitant cleavage of C<sub>6</sub>-C<sub>4'</sub> bond to give the products. In the product complex, the unpaired electron is localized on C<sub>6'</sub> with  $\rho(C_6') = 0.80$ . Because the location of highest spin density changes from C<sub>4</sub> in the starting material to C<sub>5</sub> in the intermediate, it is reasonable to

(45) Orlov, V. M.; Smirnov, A. N.; Varshavsky, Y. M. *Tetrahedron Lett.* **1976**, 4377-4378.

(46) Hush, N. S.; Cheung, A. S. *Chem. Phys. Lett.* **1975**, 34, 11-13.

**Table 6.** PM3-Calculated Charges of the Pyrimidine Fragments at Various Stationary Points in the Fragmentation of the Radical Anion of the Oxetane and Azetidine Isomers

		Thy[ox]Thy <sup>-</sup>		Thy[az]Cyt(Z) <sup>-</sup>		Thy[az]Cyt(E) <sup>-</sup>	
		q <sub>5'</sub>	q <sub>3'</sub>	q <sub>5'</sub>	q <sub>3'</sub>	q <sub>5'</sub>	q <sub>3'</sub>
path a	SM	-0.108	-0.892	-0.872	-0.128	-0.211	-0.789
	TS1	-0.581	-0.419	-0.722	-0.278	-0.702	-0.298
	int	-0.270	-0.73	-0.821	-0.179	-0.821	-0.179
	TS2	-0.384	-0.616	-0.584	-0.416	-0.578	-0.422
	complex	-0.058	-0.942	-0.125	-0.875	-0.121	-0.879
path b	SM	-0.108	-0.892	-0.872	-0.128	-0.211	-0.789
	TS1	-0.666	-0.334	-0.862	-0.138	-0.234	-0.766
	int	-0.192	-0.808	-0.923	-0.0077	-0.324	-0.676
	TS2	-0.358	-0.642	-0.232	-0.768	-0.394	-0.606
	complex	-0.323	-0.677	-0.113	-0.887	-0.325	-0.675

expect that the unpaired electron becomes more delocalized in the transition state leading to the intermediate. This is, indeed, reflected in the calculated spin densities:  $\rho(C_4) = 0.27$ ,  $\rho(O_4) = 0.27$ ,  $\rho(C_5) = 0.14$ ,  $\rho(O_4') = 0.26$ , and  $\rho(C_6') = 0.23$ . In the cation radical pathway, however, the unpaired electron is centered on C<sub>5'</sub> with  $\rho(C_5') = 0.72$  (see Figure 7c). This unpaired electron is in a position to form a  $\pi$  bond with C<sub>4'</sub> with concomitant cleavage of C<sub>6</sub>-C<sub>4'</sub> bond. In the intermediate, the spin density is centered on C<sub>6</sub>, which may induce the formation of a  $\pi$  bond with the adjacent C<sub>5</sub> with concomitant cleavage of C<sub>5</sub>-O<sub>4'</sub> bond. PM3 calculations gave similar results (data not shown).

**Biological Implications.** Though the calculations described herein are for the gas-phase splitting of model systems for the presumed oxetane and azetidine intermediates, they can give some insight into possible enzymatic pathways. One important feature of the photoenzymatic mechanism is that both T[6-4]T and T[6-4]C are repaired by (6-4) photolyase with similar efficiencies.<sup>12</sup> Based on the gas-phase results alone, one might conclude that the photoenzymatic mechanism could not proceed by either an anion or a cation radical mechanism, because the azetidine substrate always has a higher rate-determining barrier than the oxetane substrate. There is evidence, however, that a reduced flavin cofactor is involved, suggesting that the enzyme does catalyze the splitting through the formation of anion radical intermediates.<sup>19</sup> If so, either the enzyme must be lowering the barrier of splitting of the azetidine intermediates, or it must be catalyzing the reversal of the (6-4) products by some other mechanism, though such a mechanism is hard to conceive. The enzyme could conceivably lower the barrier for splitting of the azetidine intermediate by simply solvating or protonating N<sub>4</sub>. To test this idea, we also examined the reversal of the protonated azetidine intermediate Thy[az]CytH<sup>+</sup> (Figure 5c) upon addition of an electron to produce a neutral radical intermediate. Though we were able to obtain a stable structure for the protonated azetidine intermediate, all attempts to find a minimized structure for the neutral radical failed, and only the intermediate in which the C<sub>5</sub>-N<sub>4</sub> bond was cleaved (path a) could be obtained. This result contrasts with those recently reported for the effect of proton transfer to and from anion and cation radicals of *cis,syn* cyclobutane pyrimidine dimers, which has been found to increase the barriers in the gas phase.<sup>47</sup> In addition to lowering the barrier for the first step in splitting of the anion radicals, protonation or hydrogen bonding by the (6-4) photolyase to the oxetane oxygen could also be used to steer the splitting along pathway a, so as to avoid a possibly high second barrier that is found to occur with path b (Figure 8a).

**Table 7.** Energies (kcal/mol) and N<sub>3</sub>-C<sub>6</sub> Bond Lengths of the Intermediates in the Gas-Phase Fragmentation of the Dewar Pyrimidone Model Calculated by PM3

	$\Delta H_f$	$\Delta H^\ddagger$	$\Delta H_{rxn}$	N <sub>3</sub> -C <sub>6</sub>		
				SM	TS	product
Dewar (neutral)	27.8	30.1	-45.9	1.56	1.93	2.83
Dewar (radical anion)	12.6	7.9	-63.5	1.57	1.81	2.84
Dewar(radical cation)	230.2	20.6	-52.6	1.57	2.03	2.81

We also calculated the transition states for splitting of the radical anion of Cyt[ox]Thy by path a and found that its first barrier was intermediate between that of the radical anion of Thy[ox]Thy and either stereoisomer of Thy[az]Cyt (Table 3). The first barrier was considerably lower, however, for the anion radical of the *E*-imino isomer, Cyt(*E*)[ox]Thy, which would suggest that the enzyme might be able to lower the first barrier for this substrate by specifically binding this tautomeric form. There is evidence to suggest that the (6-4) product is not base-paired to the complementary strand but instead flips out of the duplex in binding to the (6-4) photolyase,<sup>12</sup> as has been proposed to occur for the CPD photolyase on the basis of its crystal structure.<sup>8</sup> Binding to the *E*-imino tautomer would also make sense for both the CPD and (6-4) photolyases because this tautomeric form has the same pattern of hydrogen bond donors and acceptors as does the preferred keto tautomer of thymine (see Figure 1). This could explain how the (6-4) photolyase could recognize and bind the photoproducts of TT, TC, CT, and CC and their respective oxetane and azetidine isomers. A similar argument could be made for the *cis,syn* cyclobutane pyrimidine dimers. In this regard, previous calculations of the splitting of C-containing CPDs have focused only on the amino tautomers. When we calculate the transition states for splitting of the radical anion of the *E*-imino tautomer of the CPD of CC, Cyt(*E*)[*c,s*]Cyt(*E*), by AM1 for the preferred pathway, we find that the first barrier drops from 16.2 to 7.5 kcal/mol. Thus, it may be important to consider that both the CPD and (6-4) photolyases bind and repair C-containing photoproducts in their *E*-imino tautomeric forms.

As pointed out in the Introduction, one motivation for considering a common mechanism for reversal of CPDs and (6-4) products was that the CPD and (6-4) photolyases share the same cofactors and highly homologous protein sequences. Experimentally, the quantum yields for the photoreactivation by *Escherichia coli* CPD photolyase and by *Xenopus laevis* (6-4) photolyase, which both contain only the fully reduced flavin, are 0.42 and 0.11, respectively.<sup>11</sup> In comparison, the AM1 activation energies for the first and second step in splitting of the Thy[ox]Thy by path a are 3.6 and 1.0 kcal/mol, whereas the corresponding activation energies for the splitting of Thy-[*c,s*]Thy are 4.7 and 5.3 kcal/mol, respectively.<sup>20</sup> Though this would appear to predict that reversal of the (6-4) products would be more efficient, it does not take into account the fact that the (6-4) products first have to be isomerized to their oxetane or azetidine isomers, which is expected to be unfavorable. In contrast, no such isomerization step is required for the reversal of CPDs.

It was also observed that the (6-4) photolyase could reverse Dewar products to the parent nucleotides, though much less efficiently (0.3%).<sup>12</sup> On the basis of the gas-phase results, the Dewar product can be converted by both anion and cation radical mechanisms to the (6-4) product (Table 7), which could be subsequently repaired. Whereas the barrier for conversion of the Dewar product to the (6-4) product via the anion radical mechanism is low (7.9 kcal/mol) and only a few kilocalories

(47) Rak, J.; Voityuk, A. A.; Michel-Beyerle, M.-E.; Roesch, N. *J. Phys. Chem. A* **1999**, *103*, 3569-3574.

per mole higher than that for reversal of the oxetane intermediate, the barrier for reversal of the cation radical intermediate is much higher. The inefficient enzymatic reversal of the Dewar product could then be explained by a combination of a higher intrinsic barrier and the fact that the enzyme evolved to lower the barrier for splitting of oxetane and azetidines and not Dewar products.

### Conclusions

The stationary points on the potential energy surfaces for the gas-phase splittings of Thy[ox]Thy and both stereoisomers of Thy[az]Cyt for both the anion radical and cation radical pathways have been located by semiempirical AM1 and PM3 methods. The results suggest that, in the gas phase, anion radical pathway works best for reversing both classes of intermediates, though a protein environment, where selective solvation and protonation can occur, is likely to be required to steer the

reaction along this pathway and lower the otherwise higher rate-determining barrier for the azetidine substrate.

**Acknowledgment.** This work was supported by NIH CA-40463 and a generous allocation of computational time from the Chemistry Computer Facility. We also thank Omar El-Ghazzawy of the Chemistry Computer Facility for help and Dr. Jianguo Yu at Wavefunction Inc. for carrying out two of the transition-state calculations.

**Supporting Information Available:** Plots of the HOMO and electrostatic potential for the stationary points in the splitting of the radical anions of Thy[ox]Thy and Thy[az]Cyt(Z) by path a, and the splitting of the cation radicals of Thy[ox]Thy and Thy[az]Cyt(Z) by path b (PDF). This material is available free of charge via the Internet at <http://pubs.acs.org>.

JA992244T